Available online at www.sciencedirect.com
ScienceDirect
Physics Letters B 650 (2007) 119–123
PHYSICS LETTERS B
www.elsevier.com/locate/physletb

Density and geometry of single component plasmas

ATRAP Collaboration

A. Speck [a], G. Gabrielse [b,*], P. Larochelle [b], D. Le Sage [b], B. Levitt [b], W.S. Kolthammer [b], R. McConnell [b], J. Wrubel [b], D. Grzonka [c], W. Oelert [c], T. Sefzick [c], Z. Zhang [c], D. Comeau [d], M.C. George [d], E.A. Hessels [d], C.H. Storry [d], M. Weel [d], J. Walz [e]

[a] *Rowland Institute at Harvard University, Cambridge, MA 02142, USA*
[b] *Department of Physics, Harvard University, Cambridge, MA 02138, USA*
[c] *IKP, Forschungszentrum Jülich GmbH, 52425 Jülich, Germany*
[d] *York University, Department of Physics and Astronomy, Toronto, Ontario M3J 1P3, Canada*
[e] *Institut fur Physik, Johannes Gutenberg-Universität, D-55099 Mainz, Germany*

Received 4 February 2007; received in revised form 26 March 2007; accepted 31 March 2007

Available online 4 April 2007

Editor: L. Rolandi

Abstract

The density and geometry of $\bar{p}$ and e^+ plasmas in realistic trapping potentials are required to understand and optimize antihydrogen ($\bar{\mathrm{H}}$) formation. An aperture method and a quadrupole oscillation frequency method for characterizing such plasmas are compared for the first time, using electrons in a cylindrical Penning trap. Both methods are used in a way that makes it unnecessary to assume that the plasmas are spheroidal, and it is shown that they are not. Good agreement between the two methods illustrates the possibility to accurately determine plasma densities and geometries within non-idealized, realistic trapping potentials.

Two methods now produce slow antihydrogen ($\bar{\mathrm{H}}$). The first method, used most often, produces $\bar{\mathrm{H}}$ in a nested Penning trap [1] during the positron cooling of antiprotons [2]. $\bar{\mathrm{H}}$ formation is established by either detecting $\bar{\mathrm{H}}$ field ionization [3,4] or by detecting $\bar{p}$ annihilation and e^+ annihilation in coincidence [5]. A second $\bar{\mathrm{H}}$ production method [6], uses lasers to control a two-step charge exchange process [7]. Common to both methods are single component plasmas of $\bar{p}$ and e^+—the density and geometry of which must be determined reliably if the $\bar{\mathrm{H}}$ production is to be understood and optimized.

In this Letter two very different methods to determine the density and spatial profile of single component plasmas are compared for the first time. Electrons are used as a more readily available substitute for e^+ plasmas. One method utilized the charge deposited when the plasma is sent through an aperture [8]. Here we collect charge on a central disk and two apertures that precede it (Fig. 1(d)), and correct for a small angle θ between the trap axis and the magnetic field direction. The second method is measuring a frequency of a quadrupole oscillation of the plasma [9–14].

We use both methods in an extended form that avoids relying upon the simplifying assumption that the plasmas have a spheroidal shape, an assumption that is valid only when the single component plasma is located within a pure electrostatic quadrupole. This assumption is sometimes made (e.g. [15,16]) because the plasma characterization is greatly simplified by internal oscillation frequencies of spheroidal plasmas that are known analytically [9,10]. However, the extended plasmas we use within cylindrical trap electrodes are not located within a pure quadrupole potential, and are thus a good test of the two generalized methods. For the aperture method we self-consistently solve Maxwell's and Poisson's equations assuming thermal equilibrium to determine the plasma geometries and densities for potentials actually applied to the trap elec-

* Corresponding author.
E-mail address: gabrielse@physics.harvard.edu (G. Gabrielse).

0370-2693/$ – see front matter
doi:10.1016/j.physletb.2007.03.054

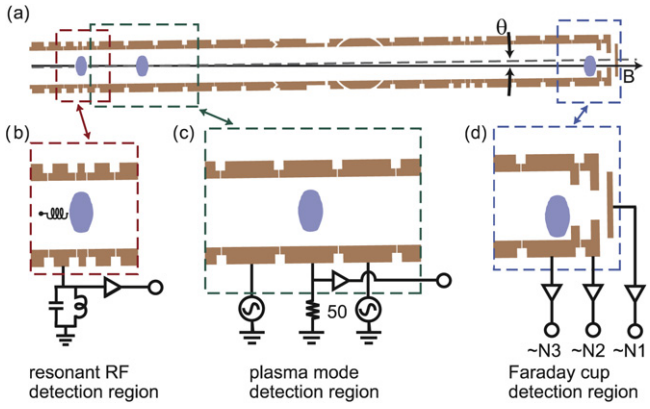

Fig. 1. Overview of the trap electrodes (a) and detection methods ((b)–(d)) used to characterize single component plasmas. A non-destructive resonant technique (b) measures the number of particles in a plasma. A non-destructive technique based on plasma modes (c) and a destructive method based on charge counting (d) determine the plasma shape and density.

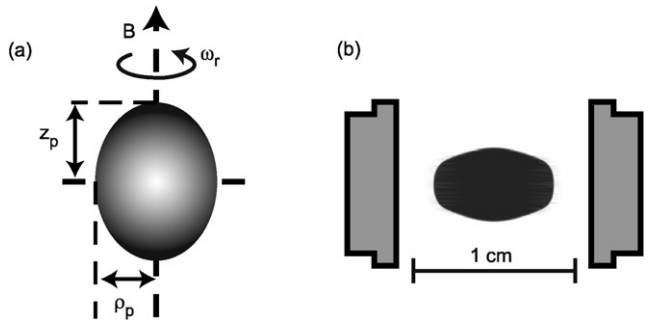

Fig. 2. Plasmas in (a) an ideal Penning trap with quadrupole electric field and in (b) an actual cylindrical electrode. For $T > 0$ the plasma half-length and radius are taken to correspond to density $n_0/2$.

trodes [17]. For the quadrupole oscillation frequency method, we use particle-in-a-cell methods to determine the frequency of oscillations around this equilibrium density and geometry [18,19]. While the possible effect of realistic potentials has been considered separately for the aperture method [8] and for the quadrupole oscillation method [13,18], this is the first test of whether the two very different methods give consistent plasma characterizations.

Traps for confining e^- are formed by biasing a stack of 38 cylindrical electrodes (Fig. 1(a)) that are aligned as well as possible with a $B = 5.4$ T magnetic field, $B\hat{\mathbf{z}}$. The electrodes are located within a vacuum enclosure kept at 4.2 K via thermal contact with liquid helium. Plasmas of up to 10 million e^- are loaded into the trap from a field emission point. They thermally equilibrate with the 4.2 K environment via synchrotron radiation and via the damping of currents they induce in a tuned circuit that is resonant at the frequency of their oscillatory motion along the magnetic field direction. Trapped e^- are counted non-destructively using radio-frequency techniques [20] (Fig. 1(b)), and by releasing the trapped particles and measuring the charge deposited as these charges strike electrodes.

A single-component plasma with particles of charge q and mass m in an axially symmetric Penning–Malmberg trap has a thermal equilibrium density,

$$n(\rho, z) = n_0 \exp\left[-\frac{q\phi(\rho, z) + \frac{1}{2}m\omega_r(\omega_c - \omega_r)\rho^2}{kT}\right], \qquad (1)$$

in cylindrical coordinates. This Maxwell–Boltzmann distribution for temperature T rigidly rotates around the magnetic field axis $\hat{\mathbf{z}}$ at a frequency ω_r [10]. Here, n_0 is the central density and $\omega_c = qB/m$ is the free-space cyclotron frequency. The electrostatic potential $\phi(\rho, z)$ is the combined potential of the external trap along with the self-potential of the plasma—a self-consistent solution of Poisson's equation: $\nabla^2\phi(\rho, z) = -qn(\rho, z)/\epsilon_0$.

For a given plasma temperature and magnetic field, the geometry and density of a trapped plasma in a Penning–Malmberg trap is thus fully determined by two parameters—the central density n_0 and the plasma rotation frequency ω_r. Alternately, we can characterize the plasma using any two parameters that are independent combinations of these two. Options include the plasma's axial extent (z_p), radial extent (ρ_p), aspect ratio ($\alpha = z_p/\rho_p$), number of particles in the plasma (N), or alternative dynamical parameters discussed below.

For a plasma in thermal equilibrium at $T = 0$ K within the pure quadrupole potential of an idealized Penning trap, these equations result in a spheroid of constant density, n_0 (e.g. Fig. 2(a)). For $T > 0$ K, the density at the boundary of the spheroid goes to zero over a Debye length. Any departure from a quadrupole potential distorts the plasma shape away from a spheroid (e.g. Fig. 2(b)). A stack of ring electrodes, however they are biased, can only produce a quadrupole potential near the central axis, so non-spheroidal plasmas are certainly to be expected whenever plasmas extend over an appreciable fraction of the trap radius.

The non-ideal anharmonic trapping potential is accounted for by solving the self-consistent Maxwell–Boltzmann and Poisson equations for the combined potential of the trap and the particle charge density. We use the iterative code EQUILSOR, provided to us by Spencer [17], to calculate possible configurations of a single component plasma made up of N charged particles. To parameterize the different possible plasma configurations for a given N we choose to use the radius of the plasma ρ_p.

Measuring N and ρ_p would give us the two parameters needed to determine which of the calculated plasma distributions pertains for our plasma. Indeed, we do measure N. However, ρ_p is not so easy to measure directly. The two methods we use to characterize the density and geometry of a single component plasma are thus distinguished by what is measured as an alternative to ρ_p.

To measure N we apply a fast 6 V pulse with a rise time less than 4 ns to remove the potential well that confines the plasma. After the charged particles leave the trap, N_3 of them strike a flat electrode with a 3.56 mm aperture, N_2 pass through to strike the next flat electrode which has a 2.54 mm aperture, and N_1 pass through both apertures to strike the flat plate behind them. Positive biases prevent secondary electrons from leaving each electrode. Charge sensitive preamplifiers (Amptek A250) determine the number of charges striking each electrode (Fig. 3), and

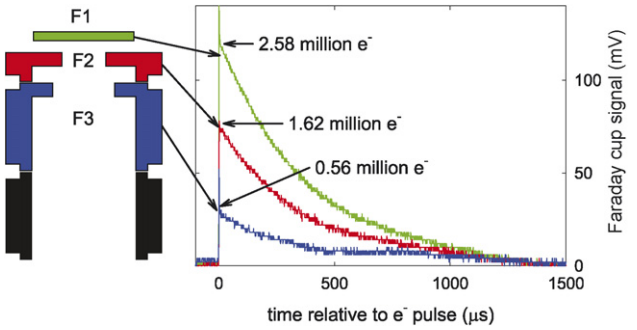

Fig. 3. Typical responses from ejecting a plasma of 4.8 million electrons onto the three Faraday cups.

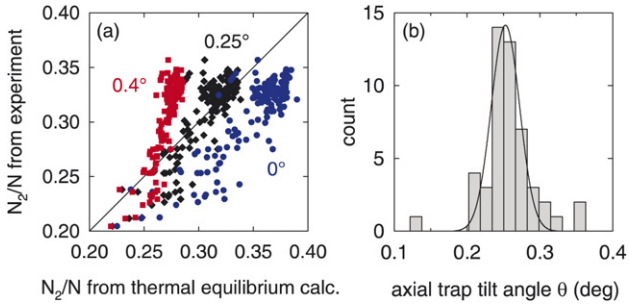

Fig. 4. (a) Comparison of the calculated Faraday cup N_2/N to the measured N_2/N for different angles of the trap axis relative to the magnetic field axis. (b) Histogram of deduced misalignments angle θ.

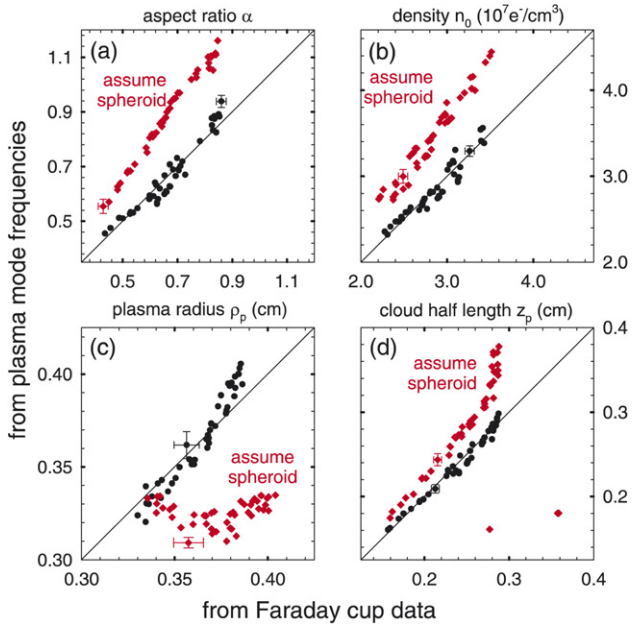

Fig. 5. (Color online.) (a)–(d) Plasma parameters measured using the plasma mode method and the segmented Faraday cup method are compared, with the diagonal line corresponding to perfect agreement. The agreement between the two methods is clearly much better when a spheroidal plasma shape (red points) is not assumed. Typical uncertainties are indicated.

$N = N_1 + N_2 + N_3$. With N determined, two measured charge ratios N_1/N and N_2/N remain to be used to characterize the plasma.

The first of the two methods that we compare makes use of these two measured charge ratios to determine the single additional plasma parameter (the plasma radius ρ_p or a more convenient alternative) that we need to fully determine the density and geometry of the plasma. Also determined is the misalignment angle θ between the electrode axis and the magnetic field. Because the released charges travel along magnetic field lines about 16.5 cm to the Faraday cups, a misalignment of only $\theta = 0.25°$ brings an on-axis particle in the plasma to a radial displacement of 0.7 mm by the time it reaches the apertures—a displacement greater than 10% of the electrode radius.

Fig. 4(a) illustrates the importance of determining the misalignment angle θ. For each plasma we measure the total number of particles, N, as discussed above. For this N we self-consistently calculate the possible 4.2 K plasma configurations using realistic trapping potentials, assuming that the e^- radiate synchrotron radiation to come into thermal equilibrium at 4.2 K. (An approximate analytical treatment of the temperature effect [21] suggests that changing the assumed temperature between 4.2 K and 0 K changes the deduced aspect ratio α by only 0.1%.) We then choose the plasma configuration that produces the observed N_1/N for each of three assumed θ values. Fig. 4(a) then compares the measured N_2/N to what is calculated for the selected plasma configuration, illustrating that one of the three small misalignment angles is better than the other two.

Since the trap misalignment does not change during our measurements we determine the best value of θ from all of our plasma samples. We use the calculated family of plasma configurations for each measured N and then iterate to find the configuration and θ that best match the measured N_1/N and N_2/N. The histogram of θ values so determined (Fig. 4(b)) is approximately a Gaussian peaked at $\theta = 0.25 \pm 0.03°$.

With this θ, the half-lengths, radii, aspect ratios and densities of the plasma configurations are redetermined from the same data by identifying the calculated plasma configuration that would best produce the measured charge ratio, N_1/N. The determined misalignment angle θ is small enough to only decrease the deduced aspect ratio by about 5% from what would be determined assuming perfect alignment for our examples.

Measured plasma characteristics are represented by the values on the x-axis and the black points in Fig. 5, which we will discuss after summarizing the quadrupole frequency method to which we compare these values. The difference between each black point and the red point directly above it in Fig. 5 is the inaccuracy that would result from assuming that the plasma is a spheroid. The typical uncertainties shown represent the reproducibility of repeated measurements (assumed independent of cloud size). The 100 kHz linewidth of the quadrupole resonance and the 5000 electron uncertainty in the Faraday cup counting account for approximately half of the uncertainty, with the remainder apparently due to variations from one loaded plasma to another.

The second method to determine single component plasma configurations requires two measured frequencies, ω_z and ω_2, along with the measured N. Possible oscillations of a spher-

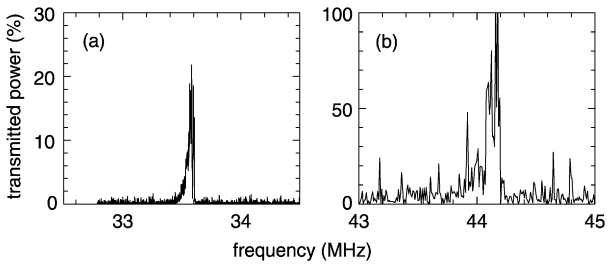

Fig. 6. Plasma response for the (a) center-of-mass mode (peaked at ω_z) and (b) quadrupole mode (peaked at ω_2).

oidal plasma are classified with integers (ℓ, m), with $\ell > 0$, $|m| < \ell$, and $m = 0$ modes being axially symmetric about $\hat{\mathbf{z}}$. The $(1, 0)$ mode is the familiar oscillation of the plasma's center of mass along $\hat{\mathbf{z}}$ that is called either the axial or bounce frequency, $\omega_z = \omega_1$. The $(2, 0)$ mode is a quadrupole mode in which the plasma aspect ratio oscillates at ω_2. The oscillation frequencies for these idealized, spheroidal plasmas are known analytically in the low temperature limit [9]. The $(\ell, 0)$ modes have frequencies, ω_ℓ, given by

$$1 - \frac{\omega_p^2}{\omega_\ell^2} = \frac{k_2}{k_1} \frac{P_l(k_1) Q_l'(k_2)}{P_l'(k_1) Q_l(k_2)}, \tag{2}$$

where

$$k_1 = \frac{\alpha}{\sqrt{\alpha^2 - 1 + (\omega_p/\omega_\ell)^2}}, \qquad k_2 = \frac{\alpha}{\sqrt{\alpha^2 - 1}}, \tag{3}$$

P_l and Q_l are Legendre functions of the first and second kind, respectively, $P_l' = dP_l(z)/dz$, $Q_l' = dQ_l(z)/dz$, and $\omega_p = \sqrt{q^2 n_0/(\epsilon_0 m)}$ is the plasma frequency.

A network analyzer (Hewlett–Packard 8753D) weakly drives two electrodes (at about −70 dBm) near the plasma (Fig. 1(c)), with the frequency range and relative phase applied to the two electrodes, as appropriate to excite ω_z and ω_2, respectively. An excited oscillation mode induces a current through a 4.2 K, 50 Ω resistor attached to the electrodes. The voltage across this resistor is amplified by +40 dB at room temperature, and is then detected by the same network analyzer. The transmission peaks when the drive is resonant with either the familiar axial frequency ω_z (Fig. 6(a)) or the quadrupole resonance frequency ω_2 (Fig. 6(b)), provided that trap and cable resonances are normalized out. Even for very low drive powers we observe particle losses at some frequencies of the drive that excites the quadrupole mode for some well depths and particle numbers, situations we avoid since these resonant effects are not yet well understood.

The equations relating ω_2/ω_z to the plasma characteristics are only approximate when realistic trapping potentials are used. Center of mass and quadrupole mode frequencies are first predicted numerically for a series of plasmas with varying number, radius, and trapping potential depth. These results are then used as a basis for interpolating the measured mode frequencies and particle numbers back to the actual plasma parameters. A self-consistent numerical calculation is performed by first calculating the equilibrium density profile for the given plasma parameters, as described above. The density profile is then perturbed to excite the quadrupole mode by axially elongating it by 1%. A Fourier transform of the center-of-mass motion and axial elongation calculated with a particle-in-cell simulation (provided by Spencer [18,19]) provides the frequencies that pertain for realistic potentials.

Fig. 5 compares the density and geometry of single component plasmas of electrons as measured using the plasma modes method and the Faraday cup aperture method. In each case, the quadrupole mode frequency was first measured, and the particles were then pulsed onto the Faraday cup apertures. The plasmas contained between 2 and 7 million e^- held at well depths between 7 and 10 V (corresponding to axial frequencies between 28 and 33 MHz). The red points illustrate the importance of using a realistic trapping potential and plasma temperature, rather than making the simplifying assumption that the plasmas are spheroidal, an assumption that only is valid for a perfect quadrupole trapping potential.

The characterization of the positron plasmas is arguably more significant for antihydrogen experiments than the distribution of antiprotons, in that a relatively small number of antiprotons is distributed within a much larger positron plasma. The measurement of antiproton plasma parameters is more challenging. This has been done using the aperture method when this method was applied in a way that allowed the nondestructive measurement of the number of antiprotons that passed through an aperture [8]. More care must be taken when all the antiprotons annihilate on the Faraday cups as would happen in this experimental configuration, since the $\bar{p}$ annihilations release charged annihilation products with high energies. With the quadrupole mode method we have not yet achieved the sensitivity required for relatively small numbers of antiprotons.

In conclusion, the density and geometry of a single component plasma that are deduced from two very different methods are compared for the first time. An aperture method and an internal oscillation frequency method agree well, even for plasmas that occupy an appreciable fraction of trapping volume within the electrodes of the Penning trap, and despite the residual misalignment of the magnetic field and the trap electrodes, which is measured. However, we explicitly show that the plasma characteristics would have been inaccurately deduced if we had made the simplifying assumption that the plasmas in the Penning trap were spheroidal. Instead, self-consistent calculations in realistic trapping potentials are used to delineate possible plasma configurations, and the frequencies of their oscillations about the equilibrium configuration. The measurements, of particle loss through an aperture, and of an oscillation frequency, then determine which of the plasma configurations pertains. The consistency between the two methods demonstrates the possibility to use either method to determine the density and geometry of single component plasmas, as is needed to quantitatively understand and optimize antihydrogen production.

Acknowledgements

We are grateful to J. Bollinger for helpful comments on the manuscript. This work was supported by the NSF and AFOSR

of the US, by the BMBF, DFG, and Jülich Laboratory of Germany, and also the NSERC, CRC, CFI and OIT of Canada.

References

[1] G. Gabrielse, S.L. Rolston, L. Haarsma, W. Kells, Phys. Lett. A 129 (1988) 38.
[2] G. Gabrielse, J. Estrada, J.N. Tan, P. Yesley, N.S. Bowden, P. Oxley, T. Roach, C.H. Storry, M. Wessels, J. Tan, et al., Phys. Lett. B 507 (2001) 1.
[3] G. Gabrielse, N.S. Bowden, P. Oxley, A. Speck, C.H. Storry, J.N. Tan, M. Wessels, D. Grzonka, W. Oelert, G. Schepers, et al., Phys. Rev. Lett. 89 (2002) 213401.
[4] G. Gabrielse, N.S. Bowden, P. Oxley, A. Speck, C.H. Storry, J.N. Tan, M. Wessels, D. Grzonka, W. Oelert, G. Schepers, et al., Phys. Rev. Lett. 89 (2002) 233401.
[5] M. Amoretti, et al., Nature 419 (2002) 456.
[6] C.H. Storry, A. Speck, D.L. Sage, N. Guise, G. Gabrielse, D. Grzonka, W. Oelert, G. Scheppers, T. Sefzick, J. Walz, et al., Phys. Rev. Lett. 93 (2004) 263401.
[7] E.A. Hessels, D.M. Homan, M.J. Cavagnero, Phys. Rev. A 57 (1998) 1668.
[8] P. Oxley, N.S. Bowden, R. Parrott, A. Speck, C. Storry, J.N. Tan, M. Wessels, G. Gabrielse, D. Grzonka, W. Oelert, et al., Phys. Lett. B 595 (2004) 60.
[9] D.H.E. Dubin, Phys. Rev. Lett. 66 (1991) 2076.
[10] J.J. Bollinger, D.J. Heinzen, F.L. Moore, W.M. Itano, D.J. Wineland, D.H.E. Dubin, Phys. Rev. A 48 (1993) 525.
[11] C.S. Weimer, J.J. Bollinger, F.L. Moore, D.J. Wineland, Phys. Rev. A 49 (1994) 3842.
[12] M.D. Tinkle, R.G. Greaves, C.M. Surko, R.L. Spencer, G.W. Mason, Phys. Rev. Lett. 40 (1994) 352.
[13] M.D. Tinkle, R.G. Greaves, C.M. Surko, Phys. Plasmas 2 (1995) 2880.
[14] M. Amoretti, et al., Phys. Plasmas 10 (2003) 3056.
[15] C.M. Surko, R.G. Greaves, M. Charlton, Hyperfine Interact. 109 (1997) 181.
[16] N. Kuroda, H.A. Torii, K.Y. Franzen, Z. Wang, S. Yoneda, M. Inoue, M. Hori, B. Juhász, D. Horváth, H. Higaki, A. Mohri, et al., Phys. Rev. Lett. 94 (2005) 023401.
[17] R.L. Spencer, S.N. Rasband, R.R. Vanfleet, Phys. Fluids B 5 (1993) 4267.
[18] G.W. Mason, R.L. Spencer, J.A. Bennett, Phys. Plasmas 3 (1996) 1502.
[19] J.K. Jennings, R.L. Spencer, K.C. Hansen, Phys. Plasmas 2 (1995) 2630.
[20] D.J. Wineland, H.G. Dehmelt, J. Appl. Phys. 46 (1975) 919.
[21] D.H.E. Dubin, Phys. Fluids B Plasma Phys. 5 (1993) 295.